DOI: 10.1002/cbdv.201800633

CHEMISTRY & BIODIVERSITY

Biological Investigations and Spectroscopic Studies of New Moxifloxacin/Glycine-Metal Complexes

Hazem S. Elshafie,[a] Shimaa H. Sakr,[a, b] Sadeek A. Sadeek,[b] and Ippolito Camele*[a]

[a] School of Agricultural, Forestry, Food and Environmental Sciences, University of Basilicata, Viale dell'Ateneo Lucano 10, 85100 Potenza, Italy, e-mail: ippolito.camele@unibas.it

[b] Department of Chemistry, Faculty of Science, Zagazig University, 44511 Zagazig, Egypt

Two novel ligand–metal complexes were prepared through the reaction of Zn(II) and Sn(II) with moxifloxacin (MOX) in the presence of glycine (Gly) to investigate their biological activities. IR, UV/VIS and ^{1}H-NMR analysis have been carried out for insuring the chelation process. Results suggested that MOX and Gly react with the metal ions through the carbonyl oxygen atom and the oxygen atom of the carboxylic group of MOX and Gly. The antimicrobial activity was carried out against some common bacterial and fungal pathogens and the radical scavenging activity (RSA%) was evaluated using DPPH and ABTS methods. Phytotoxic effect of the prepared complexes was evaluated *in vitro* against *Raphanus raphanistrum* and *Lepidium sativum*. Hemolytic activity was tested against cell membrane of erythrocytes. Results showed that the two prepared complexes exhibited high antimicrobial activity against all tested phytopathogens and no significant phytotoxic effect has been observed. Only MOX–Zn(II) complex showed moderate hemolysis at 100% concentration.

Keywords: Fluoroquinolone, spectroscopic analysis, chelation theory, metal–ligand complexes, biological activity, radical scavenging activity, antimicrobial activity.

Introduction

Great attention has recently been devoted to the synthesis of fluoroquinolone derivatives and their activity against various pathogenic microorganisms. The bactericidal activity of the fluoroquinolones is due to the inhibition of DNA gyrase and topoisomerase IV that are essential for the bacterial DNA multiplication, transcription, repair and recombination.[1]

Moxifloxacin (MOX; *Figure 1A*) with trade names Avelox, Avalox and Avelon, is one of the fourth generation fluoroquinolone antibiotics commonly used for the treatment of community and hospital-acquired infections and has a very good safety and tolerability profile.[2] MOX possesses a greater antibacterial activity than other fluoroquinolone agents such as levofloxacin and ciprofloxacin especially against Gram-positive bacteria (G+ve) and anaerobes.[3–5] MOX is active against all common community-acquired respiratory pathogens especially against *Streptococcus pneumoniae*, the typical respiratory pathogen.[3–6] On the other hand, the potency of

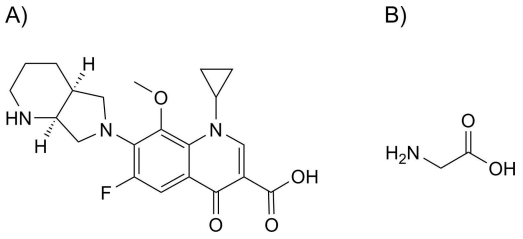

Figure 1. Structures of A) 1-cyclopropyl-6-fluoro-8-methoxy-7-[(4a*S*,7a*S*)-octahydro-6*H*-pyrrolo[3,4-*b*]pyridin-6-yl]-4-oxo-1,4-dihydroquinoline-3-carboxylic acid (MOX) and B) glycine (Gly).

MOX against members of Enterobacteriaceae family is about half of ciprofloxacin.[7,8] The *in vitro* activity of MOX against *Escherichia coli* (including highly resistant mutants) and *Staphylococcus aureus* (including resistant strains to ciprofloxacin) is better than other available quinolones such as ofloxacin, levofloxacin, sparfloxacin and trovafloxacin.[4,6]

Many research described that MOX utilized 4-carbonyl and carboxyl oxygen atoms as donor atoms

Table 1. Elemental analysis and physico-analytical data for moxifloxacin (MOX), glycine (Gly) and its metal complexes[a]

Compounds M_r and M.F.	Yield [%]	Mp. [°C]	Color	Found (calc.) [%] C	H	N	M	Cl	μ_{eff} [B. M.]	Λ S [cm^2 mol^{-1}]
MOX 401.43 ($C_{21}H_{24}N_3O_4F$)	–	240	Yellowish white	62.83 (62.78)	5.93 (5.98)	10.42 (10.46)	–	–	–	0
Gly 75.07 ($C_2H_5NO_2$)	–	233	White	31.95 (31.97)	6.62 (6.66)	18.60 (18.64)	–	–	–	50.77
(**1**) 666.49 ($ZnC_{23}H_{38}N_4O_{11}FCl$)	91	≥300	Fluorescent	41.30 (41.44)	5.65 (5.70)	8.00 (8.04)	9.58 (9.75)	5.30 (5.33)	–	86.58
(**2**) 681.71 ($SnC_{23}H_{34}N_4O_9FCl$)	97	≥300	Fluorescent	40.45 (40.52)	4.92 (4.99)	8.15 (8.22)	16.93 (17.03)	5.15 (5.20)	–	75.34

[a] M_r: molecular weight; M.F.: molecular formula; M.p.: melting point; calc.: calculated values; μ_{eff}: effective magnetic moment; S: siemens (Ohm^{-1}).

in the reaction with some metal ions.[9–13] Several *in vitro* antimicrobial assays showed that the metal–ligand complexes have higher efficacy than the parent ligands.[11,14–18]

A number of studies have concluded the interest of metal complexes and their applications in medicinal and pharmaceutical fields.[2,13,19] In addition, understanding the structure and function of the interactions with metals could avoid the side effects and increase the drug applicability.[20]

A variety of metal complexes of fluoroquinolones have been prepared and their physicochemical properties, biological and antitumor activities have been studied in comparison with free fluoroquinolones.[21–25] The biological activity of the mixed ligand complexes could be explained in many cases where enzymes are activated by metal ions.[21,22,25,26] In the literature, glycine (Gly; *Figure 1B*) has coordinated the carboxylate oxygen atom and the amino nitrogen atom in several metal–ligand complexes as a bidentate ligand.[21,25–27]

The aims of this research were to study the effect of changing atomic volume, and atomic mass of Zn(II) and Sn(II) metal ions with Cl^- as counter ion on the biological activities of MOX in the presence of Gly and to examine the mode of coordination and the biological properties of the resultant complexes.

Results and Discussion

The two complexes of MOX with Zn(II) and Sn(II) have been prepared and characterized using elemental analysis, IR, UV/VIS and ^{1}H-NMR spectra. The analytical and physical data summarized in *Table 1* indicate that the complexes are solids air stable at room temperature and contain water molecules with the molar ratio M/MOX/Gly is 1:1:1. Molar conductance of MOX and their metal complexes, measured using 1×10^{-3} mol^{-1} solutions at room temperature, was found to be in the range from 0 to 130.11 Scm^2 mol^{-1}. The data indicated that the complexes are electrolytes and the chloride ions were found as counter ions. In order to verify that the chloride is ionic in the prepared complexes, their solutions were tested with aqueous solutions of $AgNO_3$ where a white precipitate was formed. The chloride content in the complexes was determined by using two methods, i.e., Mohr's method and Volhard's Method.

IR spectra of the MOX ligand and the new complexes were used to define the structure of the prepared metal complexes and to confirm the presence of water in their composition. The IR spectra of Zn(II) and Sn(II) complexes and free MOX, Gly were obtained as KBr discs (*Figure 2*). The observed frequencies in the IR spectra of free ligands (MOX and Gly) and its complexes, their relative intensities and assignments are given in *Table 2*. The IR spectra of the prepared complexes were very similar due to the same atoms of MOX and Gly involved in the bonding to the metal. The metal ions are coordinated to a deprotonated carboxylate oxygen atom and pyridone oxygen atom of MOX and glycine through the carboxylate oxygen atom and the amino nitrogen atom. Metal ions react with MOX and Gly forming complexes of monomeric structure, in which the metal ions are six coordinate and complete the coordination number with two water molecules (*Figure 3*). The presence of the broad bands in 3560–3326 cm^{-1} range of ν(O–H) vibration in the IR spectra of the metal MOX complexes indicates the presence of water molecules in the prepared complexes. The vibration of the carboxylic stretch ν(C=O) was found at 1709 cm^{-1} as a very

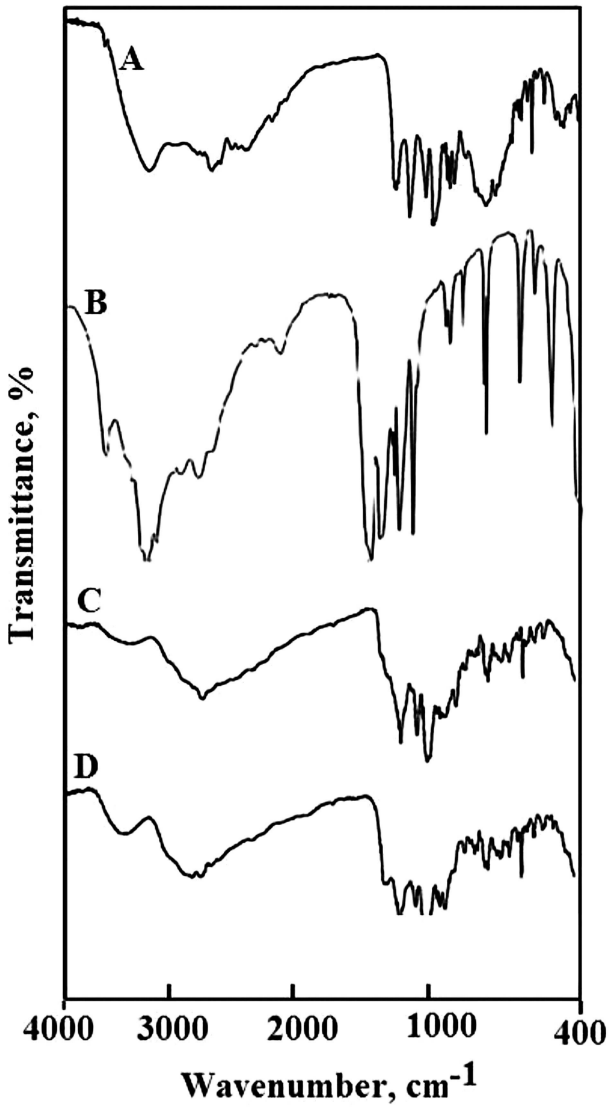

Figure 2. IR spectra of A) moxifloxacin (MOX), B) glycine (Gly), C) MOX–Sn(II) and D) MOX–Zn(II).

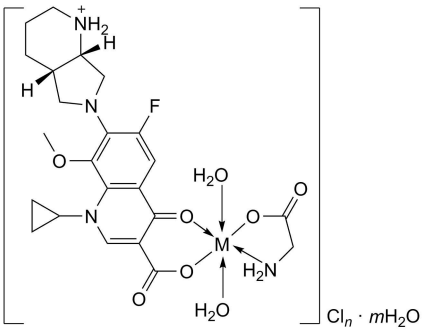

Figure 3. The coordination mode of Zn(II) and Sn(II) with mixed ligands. M = Zn(II) and Sn(II). $n = 1$ for Zn(II) and Sn(II). $m = 3$ for Zn(II) and 1 for Sn(II).

strong bond for MOX and at 1703 cm^{-1} for Gly and the pyridone stretch ν(C=O) at 1620 cm^{-1}.[28–33]

Two characteristic bands are present around 1621 and 1371 cm^{-1} with different intensities assigned to $\nu(COO^-)$ asymmetric and symmetric stretching vibrations, respectively. The difference $\Delta\nu = \nu_{as}(COO^-) - \nu_s(COO^-)$ values for complexes fall around 264 cm^{-1} indicating a monodentate coordination mode of the carboxylate group.[31–33] These changes in the IR spectra suggest that MOX and Gly are bound to metal ions via the carboxylate oxygen atom. Whereas ν(C=O) of the pyridone stretch is shifted from 1620 cm^{-1} to around 1514 cm^{-1}, being a good indication that this group is coordinated to the metal ions (*Table 2*). As regards, chelation through amino acids, the IR spectra exhibit significant features in the νNH_2 and νCOO^- regions. It is worthwhile to mention here that free amino acids exist as zwitterions and the IR spectra of these cannot be compared entirely with those of metal complexes, as amino acids in metal complexes do not exist as zwitterions. Free amino acids with NH_3^+ function in particular show νNH_3^+ at 3170 cm^{-1}. In the complexes, NH_3^+ is deprotonated and binds to metal through the neutral NH_2 group. The transformation of NH_3^+ to NH_2 must result in an upward shift in νNH_2 of free amino acids.[34–37]

The spectra of the prepared solid complexes show a group of new bands with different intensities, being characteristic for ν(M–O) and ν(M–N). The ν(M–O) and ν(M–N) bands were observed at 665, 590 and 538 cm^{-1} for Sn(II), whereas at 661, 618 and 591 cm^{-1} for Zn(II). This indicates coordination of MOX and Gly through the pyridone, the carboxylate oxygen atom of MOX, Gly and the amino nitrogen atom of Gly.

UV/VIS Spectroscopy Analysis

The chelation process can be explained using visible and UV spectroscopy which is considered as a simple and powerful tool. In a typical metal chelate, the observed spectrum, in general, consists of a series of crystal field bands, which are in the visible region and depend largely on the donor atom of the ligand on the metal ion.[33,38,39] The electronic absorption spectra of MOX along with their metal complexes are shown in *Figure 4* and the data are listed in *Table 3*. The free MOX showed bands at 326 and 406 nm which attributed to π–π^* and n–π^* transitions, respectively. The shift of the absorption bands to higher values and the appearance of new bands for the complexes are attributed to the mixed ligand complexation.

Table 2. IR frequencies (cm^{-1}) and tentative assignments for MOX, Gly, MOX–Sn(II) and MOX–Zn(II)[a]

MOX	Gly	MOX–Sn(II)	MOX–Zn(II)	Assignments
3530vs	3560vs	3441m br.	3545w	ν(O–H), H_2O, COOH
3472s	3400br	3326w	3481br.	
–	3170br.	3190w	3181br.	ν(N–H), NH_2
2733w	–	2608vw	2609w	$\nu(NH_2^+)$
2696w		2514vw	2514vw	
2635w				
2569w				
1709vs	1703s	–	–	ν(C=O), COOH
–	–	1619vs	1621vs	$\nu_{as}(COO^-)$
1620vs	1613m	1542w	1514s	ν(C=O) and δb(NH_2)
1520vs	1556m			
1358m	1401m	1371s	1371s	$\nu_s(COO^-)$
			1352vs	
691w	640m	665s	661s	ν(M–O), ν(M–N)
648 ms	621m	590w	618w	+ and ring deformation
633w	555m	538s	591s	
544s				
490vs				
424s				

[a] Keys: s = strong, w = weak, v = very, m = medium, br. = broad, ν = stretching, δb = bending.

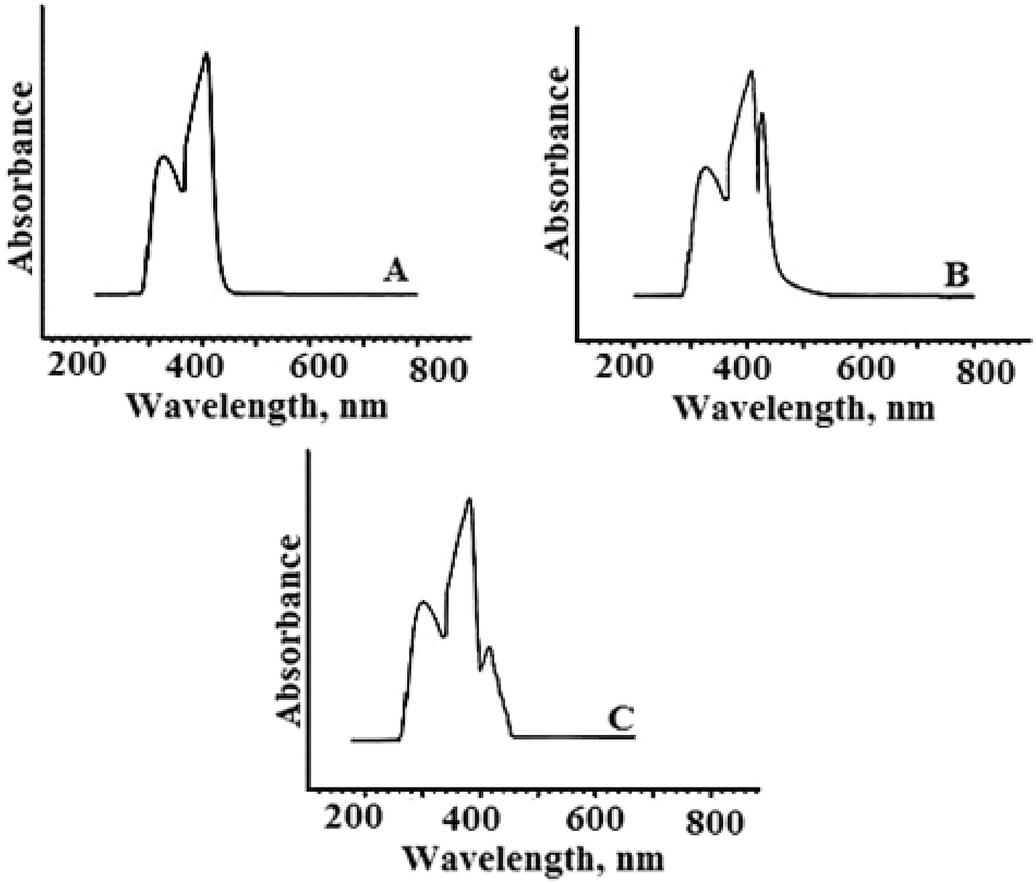

Figure 4. UV/VIS spectra of A) MOX, B) MOX–Sn(II) and C) MOX–Zn(II).

Table 3. UV/VIS spectral data of the free ligand MOX and its metal complexes

Assignments [nm]	MOX	MOX metal complexes	
		Sn(II)	Zn(II)
π–π* transitions	326	339	428
n–π* transitions	406	400	410
Ligand–metal charge transfer	–	426	460

The decrease or increase of the absorption bands and the appearance of new bands upon coordination could be caused by: i) expected increase of the metal ion mass upon coordination; ii) increase of the electron density on the metal ions by ligand and iii) decrease of the electron density on oxygen and nitrogen donor atoms. The presence of new peaks at 460 and 426 nm for Zn(II) and Sn(II) complexes attributed to complexation behavior of MOX towards metal ion,[36] which may be assigned to ligand–metal charge transfer (*Table 3*). Finally, the results presented here clearly indicated that the metal ions form stable solid complexes with the free ligands.

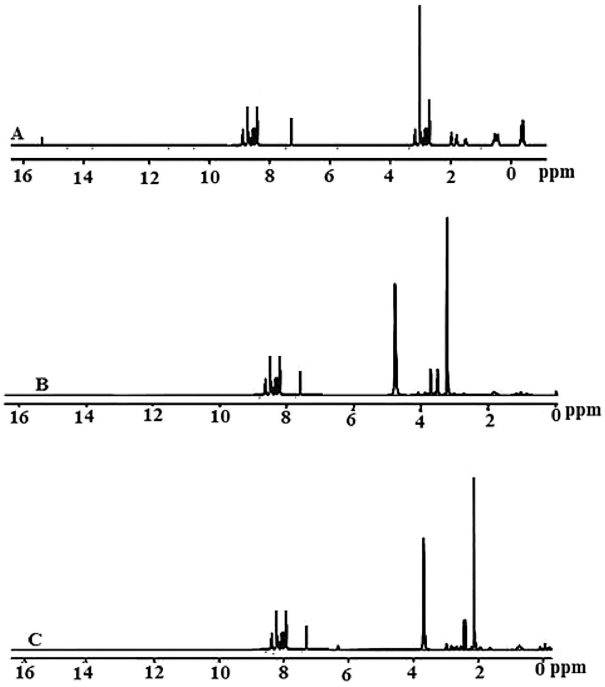

Figure 5. ^{1}H-NMR spectra of A) MOX, B) MOX–Sn(II) and C) MOX–Zn(II).

^{1}H-NMR Spectra

The NMR spectra were carried out in CD_3OD to insure the structure of the prepared metal complexes. The obtained spectra displayed distinct signals with appropriate multiplets as shown in *Figure 5*. The ^{1}H-NMR spectra of MOX and Gly showed that the Gly shows a peak at δ(H) 11.00 ppm due to the carboxylic proton. The absence of the carboxylic proton (COOH) in the spectra of complexes suggests the coordination of Gly through its carboxylate oxygen atoms. ^{1}H-NMR spectra of MOX showed signals at δ(H) 0.91 (t, $J=3.63$, H–C(1,2), 4 H); 0.02 (t, $J=7.99$, H–C(3), 4 H), 0.07 (t, $J=2.79$, H–C(10,11), 4 H), 0.02 (t, $J=7.99$, H–C(12), 1 H), 0.07 (t, $J=2.79$, H–C(13), 2 H), 0.09 (t, $J=3.59$, H–C(9), 2 H), and 3.26 (d, $J=13.03$, H–C(6), 2 H), corresponding to CH_2 of cyclopropane ring, terminal bicyclic group and piperazine protons (NH), and the singlet at δ(H) 3.89 ppm for methoxy group, and the triplet at δ(H) 0.86 (t, $J=3.43$, H–C(1′–8′), 8 H) for aromatic CH groups. The peak at δ(H) 15.12 ppm in the spectrum of MOX can be assigned to the proton of carboxylic (COOH). The resonance of the carboxylic proton (COOH) was not detected in the spectra of the two complexes, which implied the coordination of MOX through its carboxylate oxygen atoms.[29,31,40,41] The ^{1}H-NMR spectra of complexes exhibit also new peaks in the range of 4.10–4.91 ppm, due to the presence of water molecules in the complexes. On comparing the main peaks of MOX and Gly with its complexes, it is observed that all the peaks of the free ligands are present in the spectra of the complexes with chemical shift upon binding of MOX and Gly to the metal ion.

Antimicrobial Activities

The results of the antibacterial test showed that the tested ligand and its metal complexes were able to inhibit the growth of all studied bacterial strains in a dose-dependent manner (*Figure 6*). All prepared MOX–metal complexes showed the highest significant activity against *E. coli* at 10000 μg ml^{-1} compared to the two tested antibiotics used as controls followed by the parent ligand at 10000 μg ml^{-1} and MOX–Zn(II) at 1000 μg ml^{-1}, whereas MOX at 1000 μg ml^{-1} and MOX–Sn(II) at 1000 μg ml^{-1} showed moderate antibacterial activity against the above bacteria. Finally, free MOX ligand at 100 μg ml^{-1} and MOX–Sn(II) at 100 μg ml^{-1} showed the lowest significant activity against *E. coli*. On the other hand, free MOX ligand and all its metal complexes were able to significantly inhibit the growth of *C. michiganensis* at all tested concentrations compared to the two tested antibiotics. In the case of *X. campestris*, the MOX–Zn(II) complex at 10000 μg ml^{-1} showed the highest significant activity,

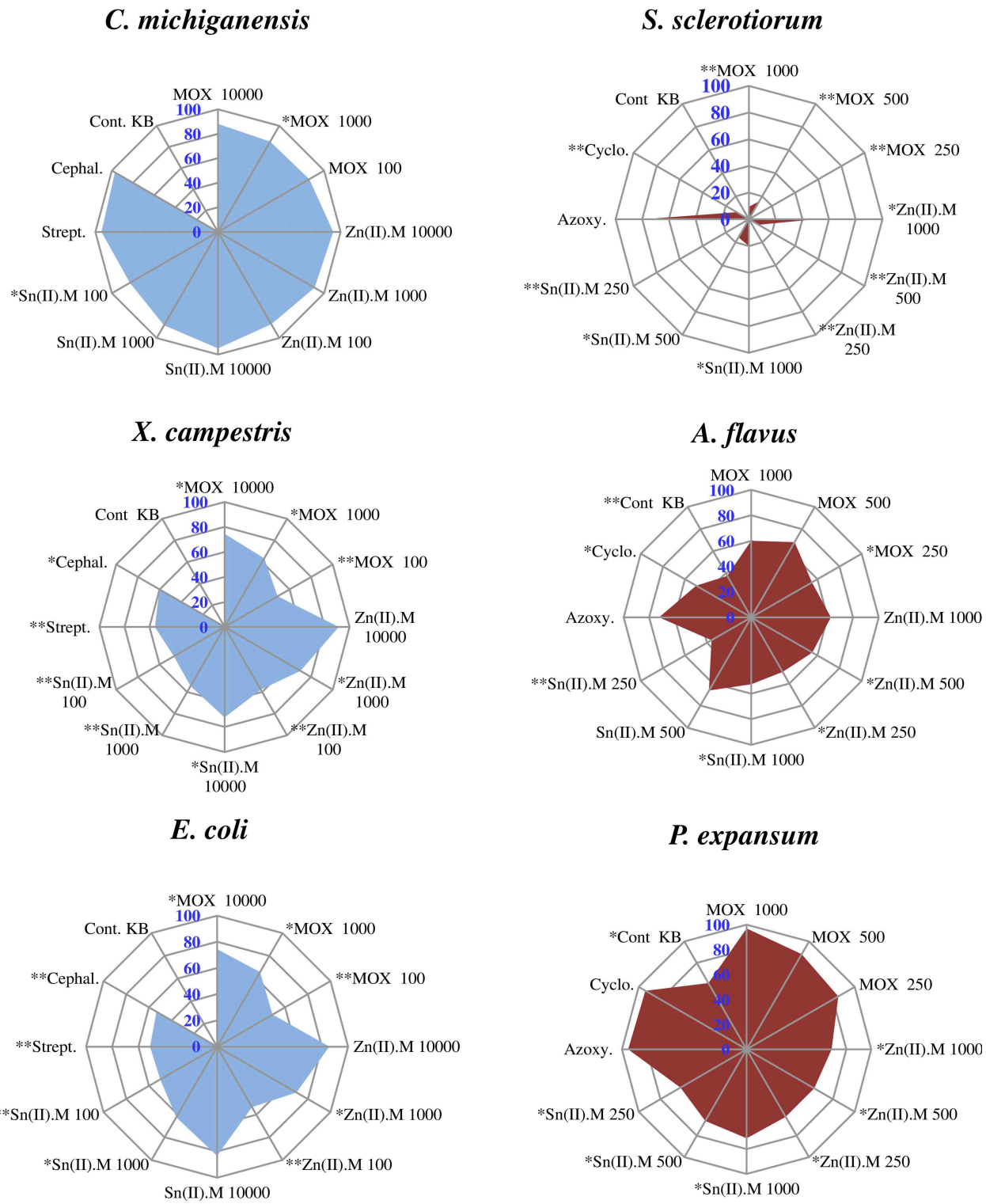

Figure 6. Antimicrobial activity of moxifloxacin and its metal complexes. MOX: Moxifloxacin, Zn(II).M: Zinc.Mox complex; Sn(II).M: Tin.Mox complex; Strept.: Streptomycin 50 μg/ml; Cephal.: Cephaloxacin 30 μg/ml; Azoxy.: Azoxystrobin 1 μl/ml; Cyclo.: Cycloheximide 0.1 μl/ml. Values are recorded as the mean of growth inhibition percentage from three replicates ± SD. *: Statistically significant at $P < 0.05$. **: Statistically significant at $P < 0.01$.

whereas MOX at 100 μg ml^{-1} and MOX–Sn(II) at 100 μg ml^{-1} showed the lowest significant activity against *X. campestris* (*Figure 6*).

The possible fungicidal activity of MOX and its metal complexes was determined against three serious phytopathogens (*S. sclerotiorum*, *A. flavus* and *P. expansum*). In particular, results of *in vitro* antifungal activity against *S. sclerotiorum* and *A. flavus* explicated that Azoxystrobin has the highest significant activity followed by MOX–Zn(II) and MOX–Sn(II) complexes at the highest concentration (*Figure 6*). The results of antifungal activity against *P. expansum* showed that uncomplexed MOX ligand at 1000 μg ml^{-1} and the two synthetic fungicides have the highest significant activity compared to all other treatments (*Figure 6*).

Mode of Action

The enhancement of antimicrobial activity of some metal–ligand complexes is based on the structures of ligand themselves. In addition, the chelation process between the ligands and the metals may reduce the polarity of the metal ion by sharing its positive charge with the donor groups and possibly the π-electron delocalization within the whole chelate ring system.[30,42] On the other hand, MOX differs structurally from other fluoroquinolones in the methoxy function at the C(8) position and an (*S*,*S*)-configured diazabicyclononyl ring moiety at the C(7) position.[43] Mitscher et al.[44] reported that the cyclopropyl group at the N(1) position and the fluorine group at the C(6) position of MOX ligand can effectively enhance its antimicrobial activity. Due to the possible mechanism of chelation process discussed above, the permeability of microbial cells might be increased due to the high lipophilic nature of the metal complexes. The penetration of those new complexes may be increased into the lipid layer of the cell membrane of microorganisms, which in turn leads to the microbial growth inhibition and probably the complete cell death.[41–45]

Antioxidant Activity

Results showed that the RSA% values of MOX–Sn(II) complex by using DPPH and ABTS assays were 95.00 and 90.68 %, respectively, compared to all other treatments. In any case, ABTS was considered as the most sensitive method, since it is characterized by higher repeatability, detectability and sensibility than DPPH assay, which was affected by several aspects, such as the type of solvents (methanol, ethanol, etc.), concentration of working solutions, ratio between volumes of sample/reagent, duration of reaction, wavelength of measuring absorbance and standard solutions.[46] The two utilized assays did not show any significant differences regarding the RSA% value of the two tested metal complexes.

The highest antiradical activity of MOX–Sn(II) complex may be correlated to its hydrogen donating ability as discussed by Corona-Bustamante et al.[47] and Sakr et al.[48] It is of interest to refer to the possible relation between the high antioxidant activity of MOX–Sn(II) complex and its low antimicrobial activity where the oxygenated compounds, in general, can attribute to the destroying of the microbial cell wall composition and thus increase the permeability of cytoplasm fluid.[42,49] Few studies showed that there is a sort of correlation between antioxidant and antimicrobial capacities of different substances. The obtained results of the current research were able to clarify this correlation, where the high oxidative compounds have the ability to interrupt the microbial cell membrane by reducing the free radicals from its surface and hence to increase the cell permeability which in turn inhibit the cell growth.[48]

Phytotoxicity Assay

The phytotoxic effect of MOX ligand and the prepared metal complexes was performed against *R. raphanistrum* and *L. sativum* and the results are listed in *Table 4*. All tested concentrations of prepared complexes and the free ligand affected SG and RE of the above mentioned tested plants in a different manner. In particular, the highest dose of MOX–Sn(II) (14.12 mg/ml) and MOX–Zn(II) (12.42 mg/ml) have significantly prevented SG and RE of *R. raphanistrum*. The same doses significantly reduced the SG and RE of *L. sativum* (*Table 4*).

On the other hand, there is no significant phytotoxic effect between the control and MOX at 1.87 mg/ml and MOX–Zn(II) at 3.11 mg/ml concentrations against *L. sativum*. However, there is no significant phytotoxic effect between the control and MOX–Zn(II) at 3.11 mg/ml concentration against *R. raphanistrum* (*Table 4*). Results showed also that there is little significant difference between the control and MOX–Sn(II) at 3.53 mg/ml concentration in the case of *L. sativum* and between MOX and MOX–Sn(II) at 1.87 mg/ml and 3.53 mg/ml concentrations, respectively, in the case of *R. raphanistrum* (*Table 4*).

The obtained results gave a good insight for the possible use of the new prepared metal complexes of MOX ligand for safely controlling different phytopath-

Table 4. Phytotoxicity effect of free MOX ligand, MOX–Sn(II) and MOX–Zn(II) complexes[a]

	Concentration [mg/ml]	Seed germination [n]	Radicle elongation [cm]	Germination index [%]
L. sativum	MOX.i	8 ± 0.52ab	0.69 ± 0.16b	11.67bc
	MOX.ii	8 ± 0.52ab	1.85 ± 0.67ab	31.22b
	MOX.iii	10 ± 0.52a	2.69 ± 0.44ab	61.22a
	MOX–Sn.i	3 ± 0.52b	0.50 ± 0.35b	3.67c
	MOX–Sn.ii	6 ± 0.52ab	0.85 ± 0.56b	11.85bc
	MOX–Sn.iii	11 ± 0.89a	2.28 ± 1.00ab	55.29ab
	MOX–Zn.i	5 ± 0.52b	0.50 ± 0.42b	5.14c
	MOX–Zn.ii	7 ± 0.52ab	1.22 ± 0.95b	19.64b
	MOX–Zn.iii	10 ± 0.52a	3.14 ± 0.90a	71.46a
	Control (H_2O)	11 ± 0.89a	4.13 ± 1.02a	99.88a
R. raphanistrum	MOX.i	4 ± 1.37b	0.70 ± 0.38b	7.23bc
	MOX.ii	6 ± 1.79a	1.12 ± 0.31b	18.87b
	MOX.iii	7 ± 0.89a	2.62 ± 0.52ab	51.60ab
	MOX–Sn.i	0 ± 0.00c	0.00 ± 0.00c	0.00c
	MOX–Sn.ii	4 ± 0.89b	1.94 ± 0.74ab	21.88b
	MOX–Sn.iii	5 ± 1.37ab	4.03 ± 0.56a	60.60ab
	MOX–Zn.i	0 ± 0.00c	0.00 ± 0.00c	0.00c
	MOX–Zn.ii	4 ± 1.37b	2.20 ± 0.47ab	22.72b
	MOX–Zn.iii	6 ± 1.86a	3.94 ± 0.74a	70.33a
	Control (H_2O)	8 ± 0.52a	4.61 ± 0.80a	99.53a

[a] MOX.i: 7.5 mg/ml; MOX.ii: 3.7 mg/ml; MOX.iii: 1.87 mg/ml; MOX–Sn.i: 14.12 mg/ml; MOX–Sn.ii: 7.06 mg/ml; MOX–Sn.iii: 3.53 mg/ml; MOX–Zn.i: 12.42 mg/ml; MOX–Zn.ii: 6.21 mg/ml; MOX–Zn.iii: 3.11 mg/ml. All values are recorded as the average values of three replicates for seed germination and root elongation ± SDs. The germination index was calculated using the formula G.I. % = $[(SG_t \times RE_t)/(SG_c \times RE_c)] \times 100$. Values followed by the different letters in each vertical column for each tested plant are significantly different according to Tukey B test at $P < 0.05$.

ogens because there is no notable phytotoxic effect especially at moderate and low concentrations (*Table 4*) against the two sensible plant species used for the bioassay test.

Hemolytic Activity

Results of hemolytic activity of the studied ligand and its metal complexes showed that the uncomplexed MOX ligand and MOX–Sn(II) did not have any hemolytic activity at all tested concentrations, whereas, MOX–Zn(II) complex showed moderate hemolytic activity at 100% and low activity at 50 and 25% (data not shown). Therefore, the obtained results indicated that MOX–Sn(II) complex could safely be used in the pharmaceutical industry at all tested concentrations, whereas, MOX–Zn(II) complex should be manipulated with special caution only at concentrations higher than 25%.

Conclusions

The analytical and spectral data of this research have indicated that the metal ions were coordinated with MOX ligand through carbonyl oxygen atom and the oxygen atom of the carboxylic group and also through the oxygen atom of the carboxylic group and the nitrogen atom of the amine group of Gly. Results showed also that all prepared complexes exhibited higher antimicrobial activity against all target microorganisms than the parent ligand. The obtained results showed in addition that MOX–Sn(II) complex had the highest significant antioxidant activity compared to the parent ligand and MOX–Zn(II) complex and this activity could be correlated with its lower antimicrobial activity. In conclusion, the out-findings of the current research demonstrated the possibility to use the prepared metal complexes in a safe manner since they did not show any phytotoxicity and hemolytic effects.

Experimental Section

Chemicals

All chemicals used for the preparation of complexes were analytical reagent grade and were commercially available from different sources and used without further purification. MOX was purchased from Sigma (Saint Louis, USA), whereas, Gly, $AgNO_3$, K_2CrO_4 and ethanol (99.8%) were purchased from Sigma–Aldrich Company (Seelze, Germany). $SnCl_2 \cdot 2H_2O$ (98%) and $ZnCl_2$ (98%) were purchased from Carlo Erba Company (Milan, Italy).

Synthesis of MOX–Metal Complexes (Reflux Method)

The synthesis of $[Zn(MOX)(Gly)(H_2O)_2]Cl_3 \cdot 3H_2O$ and $[Sn(MOX)(Gly)(H_2O)_2]Cl \cdot H_2O$ complexes has been carried out based on the distillation technique using a reflux apparatus. The chemical reaction has been performed using ethanol as organic solvent under boiled-stirred conditions at 100 °C for 6 h. Ethanol was successively evaporated using the rotary evaporator for 30 min at 30 °C/270 rpm. The reaction has been performed by adding 0.5 mmol of each metal chloride in 50 ml of ethanol, 0.5 mmol (0.218 g) of MOX and 0.5 mmol (0.037 g) of Gly.

$[Zn(MOX)(Gly)(H_2O)_2]Cl_3 \cdot 3H_2O$ (1-Cyclopropyl-6-fluoro-8-methoxy-7-[(4a*S*,7a*S*)-octahydro-6*H*-pyrrolo-[3,4-*b*]pyridin-6-yl]-4-oxo-1,4-dihydroquinoline-3-carboxylate)(2-aminoethanoate)(bihydrate)zinc Chloride Trihydrate).

$[Sn(MOX)(Gly)(H_2O)_2]Cl \cdot H_2O$ (1-Cyclopropyl-6-fluoro-8-methoxy-7-[(4a*S*,7a*S*)-octahydro-6*H*-pyrrolo-[3,4-*b*]pyridin-6-yl]-4-oxo-1,4-dihydroquinoline-3-carboxylate)(2-aminoethanoate)(bihydrate)stannous Chloride Monohydrate).

Instruments

Molar conductance of 1×10^{-3} M solutions of ligand and metal complexes in DMF was determined at room temperature on CONSORT K410 (Turnhout, Belgium). All measurements were carried out at ambient temperature with freshly prepared solutions. Melting points were recorded on a Büchi apparatus.

Electronic spectra were obtained using a T80 UV/VIS spectrometer (Taylors, USA). Magnetic susceptibilities of the powdered samples were determined on a Sherwood scientific magnetic balance (Cambridge, UK) using the Gouy method with $Hg[Co(SCN)_4]$ as calibrant.

IR spectra were recorded in KBr discs using an FT/IR-460 Plus model Jasco-32 spectrophotometer (Easton, USA) in the range from 4000 to 400 cm^{-1}. The data were analyzed using spectra manager software program at the Department of Science, Basilicata University, Potenza, Italy. The reading was elaborated considering the sample transmission, wavelength 4 cm^{-1} and the scanning cycle number between 50 and 150 according to each sample concentration.

^{1}H-NMR spectra were recorded on a Varian 400 NMR spectrometer (Illinois, USA) using CD_3OD as solvent; δ in ppm relative to Me_4Si as internal standard, J in Hz. The spectrometer was equipped with a 5 mm direct detection pulsed field z-axis gradient probe, operating at 399.96 MHz for ^{1}H and 128 scans were acquired for each experiment.

Elemental C, H, N analysis was carried out on PerkinElmer CHN 2400 (Waltham, USA). The percentage of metal ions was determined by using the atomic absorption method with a PYE-UNICAM SP 1900 spectrometer (Cambridge, England) fitted with the corresponding lamp.

Antimicrobial Investigations

The tested bacterial strains were *Clavibacter michiganensis* Smith, *Xanthomonas campestris* Pammel and *E. coli* Migula, which were listed in National Collection of Plant Pathogenic Bacteria Catalogue (NCPPB) and have been conserved as pure cultures in the collection of the School of Agricultural, Forestry, Food and Environmental Sciences, University of Basilicata, Potenza, Italy. The tested phytopathogenic fungi were *Sclerotinia sclerotiorum* (Lib.) de Bary., *Aspergillus flavus* Link ex Gray. and *Penicillium expansum* Link were previously identified using morphological and molecular methods.

In Vitro *Assays*. The disc diffusion method has been carried out for the antibacterial test.[49,50] The bacterial suspension of each strain was prepared in sterile distilled water incorporated in soft agar (0.7%) adjusted by Turbidimetry (Biolog, USA) at 10^8 colony form unit (CFU)$\cdot$$mL^{-1}$ corresponding to 0.2 nm optical density (OD). Four mL of soft agar and bacterial suspension (9:1, *v/v*) were poured into Petri dish (ϕ 90 mm) containing 10 ml KB media. Blank discs (ϕ

6 mm; OXOID, Milan, Italy) were placed over KB-plate surfaces and 20 μL from each ligand and metal complexes aliquots were applied over the discs at the following concentrations: 10000, 1000 and 100 μg/ml. Streptomycin and cephaloxacin were used as positive controls at 50 $\mu g\,ml^{-1}$ and 30 $\mu g\,ml^{-1}$, respectively, based on the medical or veterinary assays. All plates were incubated at 37 °C for 24 h and the bactericidal activity has been evaluated by measuring the growth inhibition percentage. All tested treatments have been carried out in triplicates.

For antifungal activity assay, three concentrations (1000, 500 and 250 μg/ml) of each treatment were prepared in Potato Dextrose Agar (PDA) following the incorporation method reported by Sofo et al.[51] and Elshafie et al.[52] Fourteen mL PDA-aliquots supplemented with each of the above-mentioned treatments were poured into Petri dishes. After that, 0.5 cm diameters of fungal disks of 96 h fresh cultures were singularly inoculated in the center of each Petri dish. All plates were incubated at 24 ± 2 °C for 4 days under dark conditions. Petri dishes containing only PDA were only inoculated with fungal disks as control. The diameter of fungal mycelium growth was measured in mm ± SDs of three replicates[53–55] and the growth inhibition percentage (GIP) was calculated using *Equation 1* by Zygadlo et al.,[56] compared to synthetic fungicides Azoxystrobin (1 $\mu L\,ml^{-1}$) and Cycloheximide (0.1 $\mu g \cdot mL^{-1}$):

$$GIP\ (\%) = 100 \times (GC - GT)/GC \quad (1)$$

where GC = average diameter of fungus grown on PDA (control), GT = average diameter of fungus grown on PDA (treated).

Antioxidant Activity

The 2,2′-azinobis(3-ethylbenzothiazoline-6-sulfonic acid) (ABTS) and 2,2-diphenyl-1-picrylhydrazyl (DPPH) assays were carried out following the principles of Martysiak-Żurowska and Wenta[46] and Elshafie et al.[49] to determine the radical scavenging activity (RSA) of the studied ligand and its metal complexes using *Equation 2*:

$$RSA\% = (1 - A_t/A_c) \times 100\,\% \quad (2)$$

Where A_t is the absorbance of each treatment and A_c is the absorbance of control sample.

DPPH Assay. This method was used for determining the antiradical activity of a compound based on the use of stable free radical DPPH. The mechanism is based on the ability of tested compounds to reduce the DPPH radical (deep violet) into a neutral stable molecule (pale yellow).[57,58] Stock radical solution of DPPH was prepared by dissolving 20 mg of DPPH in 15 ml ethanol and adjusted at 0.44 mg/ml.

Test Procedures. Fifty μL of each treatment was diluted with DPPH at 1:20 and incubated at darkness for 30 min at room temperature. All samples were centrifuged at 8000 rpm for 5 min and the absorbance was recorded at 515 nm on an UV/VIS spectrophotometer (LKB Biochrom 4050 Ultrospec II), and ethanol was used as reference sample. All determinations were carried out in triplicate.

ABTS Assay. A stock radical solution of ABTS was prepared by dissolving 38 mg of ABTS in 10 ml of an aqueous sodium persulfate solution (2.45 mM) and then was conserved in darkness for 16 h at room temperature. One ml of stock $ABTS^{\bullet+}$ solution was diluted with 29 ml of ethanol.

Test Procedures. Twenty μL of each treatment were diluted at 1:50 with $ABTS^{\bullet+}$ solution and was incubated in darkness at room temperature for 2 h. All samples were centrifuged at 8000 rpm for 5 min and the absorbance was measured at 734 nm using the above-mentioned spectrophotometer, and ethanol was used as reference sample. All determinations were carried out in triplicate.

Phytotoxicity Assay

A bioassay based on seed germination (SG) and radicle elongation (RE) was carried out to evaluate the possible phytotoxic effect of MOX ligand and the prepared metal complexes on *Raphanus raphanistrum* L. (wild radish) and *Lepidium sativum* L. (garden cress) seeds following the method reported by Ceglie et al.[59] Seeds were sterilized in 3% H_2O_2 solution for 1 min and then were rinsed twice with deionized sterile water (dH_2O). Seeds were placed either in dH_2O (control) or the above mentioned treatments and were shaken gently for 2 h. The tested concentrations were 7.50, 3.70 and 1.87 mg/ml for MOX ligand; 14.12, 7.06 and 3.53 mg/ml for MOX–Sn(II) complex and 12.42, 6.21 and 3.11 mg/ml in the case of MOX–Zn(II). The tested concentrations have been selected based on the preliminary sensibility test of each studied plant

species (data not shown). All seeds were subsequently transferred into 15 mm × 100 mm Petri dishes containing one piece of filter paper (ϕ 90 mm, Whatman No. 1). Ten seeds of each species were evenly spaced on the top of the filter paper in each Petri dish and filled with 5 ml of dH_2O or different treatments and sealed with parafilm. All Petri dishes were incubated in a growth chamber at 28 ± 2 °C with 80% relative humidity in dark conditions for 3 days. The number of germinated seeds was counted and the radical length was measured in cm. The experiment was conducted in triplicate and the germination index (GI) was calculated using *Equation 3*:

$$G.I.\% = [(SG_t \times RE_t)/(SG_c \times RE_c)] \times 100 \quad (3)$$

where GI: germination index; SG_t: average number of germinated treated seeds; RE_t: average radicle elongation for treated seeds; SG_c: average number of germinated seeds for dH_2O control; RE_c: average radicle elongation for dH_2O control. Data are expressed as the mean ± SDs for the number of germinated seeds, radicle elongation and germination index. Data were analyzed using SPSS statistical program with Tukey test at $P < 0.05$.

Hemolytic Activity

The hemolytic activity of the ligand and its prepared metal complexes was evaluated against the cell membrane of erythrocytes (RBCs) using Blood Agar Base (BAB; Oxoid) supplemented with human blood as reported by Munsch and Alatossava.[60] The blood sample was treated with heparin 25 µl 1000 U/ 5 ml blood, washed three times in buffer C (0.72 g Tris·HCl, 1.16 g NaCl, 0.07 g EDTA at pH 7) and then centrifuged at 20.000 g for 3 min at room temperature. RBCs were successively added at 0.25% to BAB and 10 ml of this suspension were poured in each Petri dish. Ten µl of each tested substance at 100, 50 and 25% were applied on BAB and incubated at 24 ± 2 °C. The hemolysis was observed as a hyaline zone after 48 h of incubation and the hemolytic activity was expressed as unit active per milliliter ($Ua\,ml^{-1}$).[61] *Pseudomonas reactans* was used as a positive-hemolytic control.[60] The whole experiment was repeated twice with three replicates.

Statistical Analysis

The results of the biological assays were statistically analyzed using the Statistical Package for the Social Sciences (SPSS; version 13.0, Prentice Hall, Chicago, IL, USA, 2004). Experimental data were expressed as mean values ± SD and comparisons were employed by Tukey post-hoc test for detecting any significant differences among different treatments at $P < 0.05$.

Acknowledgments

The authors would like to acknowledge Dr. Licia Viggiani, Dr. Agostino Galasso and Dr. Fausto Langerama, Department of Science, University of Basilicata, for their assistance in ^{1}H-NMR and IR analyses.

Author Contribution Statement

H.S.E., S.H.S. and S.A.S. designed the research study and wrote the manuscript. S.H.S. and S.A.S. carried out the spectroscopic analysis. H.S.E., I.C. and S.H.S. performed the phytotoxic and hemolytic activity assays. H.S.E and I.C. carried out the antimicrobial and antioxidant assays. I.C. and S.A.S discussed the results and revised the manuscript.

References

[1] R. A. Hauser, 'Antibiotic Basics for Clinicians: The ABCs of Choosing the Right Antibacterial Agent', 1959, 2nd edn., Wolters Kluwer, Lippincott Williams & Wilkins.

[2] A. A. Soayed, H. M. Refaat, D. A. Noor El-Din, 'Metal complexes of moxifloxacin–imidazole mixed ligands: Characterization and biological studies', *Inorg. Chim. Acta* **2013**, *406*, 230–240.

[3] A. Bauernfeind, 'Comparison of the antibacterial activities of the quinolones Bay 12–8039, gatifloxacin (AM 1155), trovafloxacin, clinafloxacin, levofloxacin and ciprofloxacin', *J. Antimicrob. Chemother.* **1997**, *40*, 639–651.

[4] M. E. Jones, M. R. Visser, M. Klootwijk, P. Heisig, J. Verhoef, F.-J. Schmitz, 'Comparative activities of clinafloxacin, grepafloxacin, levofloxacin, moxifloxacin, ofloxacin, sparfloxacin, and trovafloxacin and nonquinolones linezolid, quinupristin-dalfopristin, gentamicin, and vancomycin against clinical isolates of ciprofloxacin-resistant and -susceptible *Staphylococcus aureus* strains', *J. Antimicrob Agents Chemother.* **1999**, *43*, 421–423.

[5] S. M. El-Megharbela, A. M. A. Adama, A. S. Megaheda, M. S. Refata, 'Synthesis and molecular structure of moxifloxacin drug with metal ions as a model drug against some kinds of bacteria and fungi', *Russ. J. Gen. Chem.* **2015**, *85*, 2366–2373.

[6] H. Schedletzky, B. Wiedemann, P. Heisig, 'The effect of moxifloxacin on its target topoisomerases from *Escherichia coli* and *Staphylococcus aureus*', *J. Antimicrob. Chemother.* **1999**, *43*, 31–37.

[7] R. J. Fass, 'In Vitro Activity of Bay 12–8039, a New 8-Methoxyquinolone', *Antimicrob. Agents Chemother.* **1997**, *41*, 1818–1824.
[8] E. Pestova, J. J. Millichap, G. A. Noskin, L. R. Peterson, 'Intracellular targets of moxifloxacin: a comparison with other fluoroquinolones', *J. Antimicrob. Chemother.* **2000**, *45*, 583–590.
[9] A. J. Florence, A. R. Kennedy, N. Shankland, E. Wright, A. Al-Rubayi, 'Norfloxacin dihydrate. Acta Crystallographica Section C: Crystal Structure Communications', *Acta Crystallogr.* **2000**, *56*, 1372–1373.
[10] K. Vyas, A. Sivalakshmidevi, G. Om Reddy, 'Lansoprazole, an antiulcerative drug', *Acta Crystallogr.* **2000**, *56*, 572–573.
[11] I. Turel, 'The interactions of metal ions with quinolone antibacterial agents', *Coord. Chem. Rev.* **2002**, *232*, 27–47.
[12] N. Zhang, X. Zhang, Y. Zhao, 'Voltammetric study of the interaction of lomefloxacin (LMF)-Mg(II) complex with DNA and its analytical application', *Microchem. J.* **2003**, *75*, 249–254.
[13] K. Seku, A. K. Yamala, M. Kancherla, K. Kumar, V. Badathala, 'Synthesis of moxifloxacin–Au(III) and Ag(I) metal complexes and their biological activities', *J. Anal. Sci. Technol.* **2018**, *9*, 1–13.
[14] T. E. Spratt, S. S. Schultz, D. E. Levy, D. Chen, G. Schluter, G. M. Williams, 'Different mechanisms for the photo-induced production of oxidative DNA damage by fluoroquinolones differing in photostability', *Chem. Res. Toxicol.* **1999**, *12*, 809–815.
[15] M. Imran, T. Kokab, S. Latif, L. Mitu, Z. Mahmood, 'Synthesis, characterization and in vitro antibacterial studies of ternary complexes using quinolone antibiotics as primary ligand', *J. Chem. Soc. Pak.* **2010**, *32*, 223–228.
[16] P. Djurdjevic, L. Joksović, R. Jelić, A. Djurdjević, M. J. Stankov, 'Solution equilibria between aluminum(iii) ion and some fluoroquinolone family members. Spectroscopic and potentiometric study', *Chem. Pharm. Bull.* **2007**, *55*, 1689–1699.
[17] R. F. Grossman, J. C. Rotschafer, J. S. Tan, 'Antimicrobial treatment of lower respiratory tract infections in the hospital setting', *Am. J. Med.* **2005**, *118*, 29–38.
[18] Y. K. Kan, Y. L. Hsu, Y. H. Chen, T. C. Chen, J. Y. Wang, P. L. Kuo, 'Gemifloxacin, a Fluoroquinolone Antimicrobial Drug, Inhibits Migration and Invasion of Human Colon Cancer Cells' *BioMed Res. Int.* **2013**, *2013*, 1.
[19] H. N. Abdelhamida, H.-F. Wu, 'Monitoring metallofulfenamic–bovine serum albumin interactions: a novel method for metallodrug analysis', *Anal. Chim. Acta* **2014**, *4*, 53768–53776.
[20] H. N. Abdelhamida, H.-F. Wu, 'A method to detect metal–drug complexes and their interactions with pathogenic bacteria via graphene nanosheet assist laser desorption/ionization mass spectrometry and biosensors', *Anal. Chim. Acta* **2012**, *751*, 94–104.
[21] M. P. Lopez-Gresa, R. Ortiz, L. Perello, J. Latorre, M. Liu-Gonzalez, S. Garcia-Granda, M. Perez-Priede, E. Canton, 'Interaction of metal ions with two quinolone antimicrobial agents (cinoxacin and ciprofloxacin). Spectroscopic and X-ray structural characterization', *J. Inorg. Biochem.* **2002**, *92*, 65–74.
[22] I. Turel, A. Golobic, A. Klavzar, B. Pihlar, P. Buglyo, E. Tolis, D. Rehder, K. Sepcic, 'Interactions of oxovanadium(IV) and the quinolone family member-ciprofloxacin', *J. Inorg. Biochem.* **2003**, *95*, 199–207.
[23] B. Viossat, J. Daran, G. Savouret, G. Morgant, F. T. Greenaway, N.-H. Dung, V. A. Pham-Tran, J. R. J. Sorenson, 'Low-temperature (180 K) crystal structure, electron paramagnetic resonance spectroscopy, and propitious anticonvulsant activities of Cu^{II}_2(aspirinate)$_4$(DMF)$_2$ and other Cu^{II}_2(aspirinate)$_4$ chelates', *J. Inorg. Biochem.* **2003**, *96*, 375–385.
[24] R. N. Patel, N. Singh, K. K. Shukla, V. L. N. Gundla, U. K. Chauhan, 'Synthesis, characterization and biological activity of ternary copper(II) complexes containing polypyridyl ligands', *Spectrochim. Acta Part A* **2006**, *63*, 21–26.
[25] F. Dimiza, A. N. Papadopoulos, V. Tangoulis, V. Psycharis, C. P. Raptopoulou, D. P. Kessissoglou, G. Psomas, 'Biological evaluation of non-steroidal anti-inflammatory drugs-cobalt (II) complexes', *Dalton Trans.* **2010**, *39*, 4517–4528.
[26] E. K. Efthimiadou, M. E. Katsarou, A. Karaliota, G. Psomas, 'Copper(II) complexes with sparfloxacin and nitrogen-donor heterocyclic ligands: Structure–activity relationship', *J. Inorg. Biochem.* **2008**, *102*, 910–920.
[27] G. G. Mohamed, H. F. Abd El-Halim, M. M. I. El-Dessouky, W. H. Mahmoud, 'Synthesis and characterization of mixed ligand complexes of lomefloxacin drug and glycine with transition metals. Antibacterial, antifungal and cytotoxicity studies', *J. Mol. Struct.* **2011**, *999*, 29–38.
[28] I. Turel, N. Bukovec, E. Farkas, 'Complex formation between some metals and a quinolone family member (ciprofloxacin)', *Polyhedron* **1996**, *15*, 269–275.
[29] S. A. Sadeek, W. H. El-Shwiniy, 'Preparation, structure and microbial evaluation of metal complexes of the second generation quinolone antibacterial drug lomefloxacin', *J. Mol. Struct.* **2010**, *981*, 130–138.
[30] S. A. Sadeek, W. H. El-Shwiniy, 'Metal complexes of the fourth generation quinolone antimicrobial drug gatifloxacin: Synthesis, structure and biological evaluation', *J. Mol. Struct.* **2010**, *977*, 243–253.
[31] S. A. Sadeek, W. H. El-Shwiniy, 'Metal complexes of the third generation quinolone antibacterial drug sparfloxacin: Preparation, structure, and microbial evaluation', *J. Coord. Chem.* **2010**, *63*, 3471–3482.
[32] S. A. Sadeek, A. W. H. El-Shwiniy, W. A. Zordok, A. M. EL-Didamony, 'Spectroscopic, structure and antimicrobial activity of new Y(III) and Zr(IV) ciprofloxacin', *Spectrochim. Acta Part A* **2011**, *78*, 854–867.
[33] S. A. Sadeek, W. H. El-Shwiniy, M. S. El-Attar, 'Synthesis, characterization and antimicrobial investigation of some moxifloxacin metal complexes', *Spectrochim. Acta Part A* **2011**, *84*, 99–110.
[34] G. B. Deacon, R. J. Phillips, 'Relationships between the carbon-oxygen stretching frequencies of carboxylate complexes and the type of carboxylate coordination', *Coord. Chem. Rev.* **1980**, *33*, 227–250.
[35] K. Nakamoto, 'Infrared and Raman spectra of inorganic and coordination compounds', 4th edn., Wiley, New York, USA, 1986.
[36] G. Pasomas, A. Tarushi, E. K. Efthimiadou, 'Synthesis, characterization and DNA-binding of the mononuclear dioxouranium(VI) complex with ciprofloxacin', *Polyhedron* **2008**, *27*, 133–138.

[37] K. Nakamoto, 'Infrared spectra of inorganic and coordination compounds', Wiley Interscience, New York, USA, 1970.
[38] L. H. Abdel-Rahman, A. M. Abu-Dief, M. O. Aboelez, A. H. J. Abdel-Mawgoud, 'DNA interaction, antimicrobial, anticancer activities and molecular docking study of some new VO(II), Cr(III), Mn(II) and Ni(II) mononuclear chelates encompassing quaridentate imine ligand', *Photochem. Photobiol.* **2017**, *170*, 271–285.
[39] K. Nakamoto, P. J. McCarthy, S. FuJiwara, Y. Shimura, J. Fujita, C. R. Hare, Y. Saito, 'Spectroscopy and structure of metal chelate compounds', John Wiley & Sons, Inc., New York, London, Sydney, 1968.
[40] S. A. Sadeek, 'Synthesis, thermogravimetric analysis, infrared, electronic and mass spectra of Mn(II), Co(II) and Fe(III) norfloxacin complexes', *J. Mol. Struct.* **2005**, *753*, 1–12.
[41] I. Muhammad, I. Javed, I. Shahid, I. Nazia, 'In vitro antibacterial studies of Ciprofloxacin-imines and their complexes with Cu(II), Ni(II), Co(II), and Zn(II)', *Turk. J. Biol.* **2007**, *31*, 67–72.
[42] S. H. Sakr, H. S. Elshafie, I. Camele, S. A. Sadeek, 'Synthesis, spectroscopic, and biological studies of mixed ligand complexes of gemifloxacin and glycine with Zn(II), Sn(II), and Ce(III)', *Molecules* **2018**, *23*, 1182, 1–17.
[43] Avelox package insert, West Haven, CT, Bayer Corporation, November, 2000.
[44] L. A. Mitscher, P. Devasthale, R. Zavod, 'Structure–activity relationships', in 'Quinolone antimicrobial agents', Eds. D. C. Hooper, J. S. Wolfson, Washington DC, American Society for Microbiology, 2nd edn., 1993, pp. 3–51.
[45] N. H. Patel, H. M. Parekh, M. N. Patel, 'Synthesis, physicochemical characteristics, and biocidal activity of some transition metal mixed-ligand complexes with bidentate (NO and NN) Schiff bases', *Pharm. Chem. J.* **2007**, *1*, 78–81.
[46] D. Martysiak-Żurowska, W. Wenta, 'Comparison of ABTS and DPPH methods for assessing the total antioxidant capacity of human milk', *Acta Sci. Technol.* **2012**, *11*, 83–89.
[47] A. Corona-Bustamante, J. M. Viveros-Paredes, A. Flores-Parra, A. L. Peraza-Campos, F. J. Martínez-Martínez, M. T. Sumaya-Martínez, Á. Ramos-Organillo, 'Antioxidant Activity of Butyl- and Phenylstannoxanes Derived from 2-, 3- and 4-Pyridinecarboxylic Acids', *Molecules* **2010**, *15*, 5445–5459.
[48] V. Todorovic, M. Milenkovic, B. Vidovic, Z. Todorovic, S. Sobajic, 'Correlation between antimicrobial, antioxidant activity, and polyphenols of alkalized/nonalkalized cocoa powders', *J. Food Sci.* **2017**, *82*, 1020–1027.
[49] H. S. Elshafie, L. Viggiani, M. S. Mostafa, M. A. El-Hashash, S. A. Bufo, I. Camele, 'Biological activity and chemical identification of ornithine lipid produced by *Burkholderia gladioli* pv. *agaricicola* ICMP 11096 using LC–MS and NMR analyses', *J. Biol. Res.* **2017**, *90*, 96–103.
[50] H. S. Elshafie, L. Aliberti, M. Amato, V. De Feo, I. Camele, 'Chemical composition and antimicrobial activity of Chia (*Salvia hispanica* L.) essential oil', *Eur. Food Res. Technol.* **2018**, *244*, 1675–1682.
[51] A. Sofo, H. S. Elshafie, A. Scopa, S. M. Mang, I. Camele, 'Impact of airborne zinc pollution on the antimicrobial activity of olive oil and the microbial metabolic profiles of Zn-contaminated soils in an Italian olive orchard', *J. Trace Elem. Med. Biol.* **2018**, *49*, 276–284.
[52] H. S. Elshafie, E. Mancini, S. Sakr, L. De Martino, C. A. Mattia, V. De Feo, I. Camele, '*In vivo* antifungal activity of two essential oils from Mediterranean plants against postharvest brown rot disease of peach fruit', *J. Med. Food* **2015**, *18*, 929–934.
[53] H. S. Elshafie, N. Ghanney, S. M. Mang, A. Ferchichi, I. Camele, 'An in vitro attempt for controlling severe phyto and human pathogens using essential oils from Mediterranean plants of genus Schinus', *J. Med. Food* **2016**, *19*, 266–273.
[54] H. S. Elshafie, I. Camele, 'An overview of the biological effects of some Mediterranean essential oils on human health (Review article)', *BioMed Res. Int.* **2017**, *2017*, 1–14.
[55] H. S. Elshafie, S. Sakr, S. M. Mang, V. De Feo, I. Camele, 'Antimicrobial activity and chemical composition of three essential oils extracted from Mediterranean aromatic plants', *J. Med. Food* **2016**, *19*, 1096–1103.
[56] J. A. Zygadlo, C. A. Guzman, N. R. Grosso, 'Antifungal properties of the leaf oils of *Tagetes minuta* L. and *Tagetes filifolia* Lag', *J. Essent. Oil Res.* **1994**, *6*, 617–621.
[57] A. Bafna, S. Mishra, 'Immunomodulatory activity of methanol extract of roots of *Cissampelos pareira* Linn.', *Ars Pharm.* **2005**, *46*, 253–262.
[58] C. Cosentino, C. Labella, H. S. Elshafie, I. Camele, M. Musto, R. Paolino, P. Freschi, 'Effects of different heat treatment on lysozyme quantity and antimicrobial activity of jenny milk', *J. Dairy Sci.* **2016**, *99*, 5173–5179.
[59] F. G. Ceglie, H. S. Elshafie, V. Verrastro, F. Tittarelli, 'Evaluation of olive pomace and green waste composts as peat substitutes for organic tomato seedling production', *J. Compost Sci. Util.* **2011**, *19*, 293–300.
[60] P. Munsch, T. Alatossava, 'Several pseudomonads associated with the cultivated mushrooms *Agaricus bisporus* or *Pleurotus* sp., are hemolytic', *Microbiol. Res.* **2002**, *157*, 311–315.
[61] E. Mancini, I. Camele, H. S. Elshafie, L. De Martino, C. Pellegrino, D. Grulova, V. De Feo, 'Chemical Composition and Biological Activity of the Essential Oil of *Origanum vulgare* ssp. *hirtum* from Different Areas in the Southern Apennines (Italy)', *Chem. Biodiversity* **2014**, *11*, 639–651.

Received November 27, 2018
Accepted January 3, 2019

